Accounting for ligand-bound metal ions in docking small molecules on adenylyl cyclase toxins

ARTICLE *in* PROTEINS STRUCTURE FUNCTION AND BIOINFORMATICS · MAY 2007

Impact Factor: 2.63 · DOI: 10.1002/prot.21249 · Source: PubMed

6 AUTHORS, INCLUDING:

Deliang Chen
Changsha University of Science and Technol…
6 PUBLICATIONS **86** CITATIONS
SEE PROFILE

Johnny W Peterson
University of Texas Medical Branch at Galves…
72 PUBLICATIONS **1,379** CITATIONS
SEE PROFILE

Catherine H Schein
Foundation for Applied Molecular Evolution
114 PUBLICATIONS **2,724** CITATIONS
SEE PROFILE

PROTEINS: Structure, Function, and Bioinformatics 67:593–605 (2007)

Accounting for Ligand-Bound Metal Ions in Docking Small Molecules on Adenylyl Cyclase Toxins

Deliang Chen,[1,2] Gerd Menche,[1] Trevor D. Power,[1] Laurie Sower,[2] Johnny W. Peterson,[2,3] and Catherine H. Schein[1,2,3]*

[1]*Sealy Center for Structural Biology and Molecular Biophysics, Department of Biochemistry and Molecular Biology, University of Texas Medical Branch, Galveston, Texas 77555-0857*
[2]*Department of Microbiology and Immunology, University of Texas Medical Branch, Galveston, Texas 77555-1070*
[3]*Sealy Center for Vaccine Development, Center for Biodefense and Emerging Infections, University of Texas Medical Branch, Galveston, Texas 77555-1070*

ABSTRACT **The adenylyl cyclase toxins produced by bacteria (such as the edema factor (EF) of *Bacillus anthracis* and CyaA of *Bordetella pertussis*) are important virulence factors in anthrax and whooping cough. Co-crystal structures of these proteins differ in the number and positioning of metal ions in the active site. Metal ions bound only to the ligands in the crystal structures are not included during the docking. To determine what effect these "missing" metals have on docking results, the AutoDock, LigandFit/Cerius2, and FlexX programs were compared for their ability to correctly place substrate analogues and inhibitors into the active sites of the crystal structures of EF, CyaA, and mammalian adenylate cyclase. Protonating the phosphates of substrate analogues improved the accuracy of docking into the active site of CyaA, where the grid did not account for one of the three Mg^{2+} ions in the crystal structure. The AutoDock ranking (based on docking energies) of a test group of compounds was relatively unaffected by protonation of carboxyl groups. However, the ranking by FlexX-ChemScore varied significantly, especially for docking to CyaA, suggesting that alternate protonation states should be tested when screening compound libraries with this program. When the charges on the bound metal were set correctly, AutoDock was the most reliable program of the three tested with respect to positioning substrate analogues and ranking compounds according to their experimentally determined ability to inhibit EF. Proteins 2007;67:593–605.** © 2007 Wiley-Liss, Inc.

Key words: edema factor; *Bacillus anthracis*; CyaA; *Bordetella pertussis*; AutoDock; FlexX; ligand protonation; metal ion binding to proteins and nucleotides

INTRODUCTION

Many programs, including AutoDock,[1,2] LigandFit/Cerius2,[3] FlexX,[4–8] GOLD,[9] Glide,[10,11] and DOCK,[12] are now available to quantify possible interactions between small molecules and proteins, *in silico*. These programs can be of great value in screening large compound libraries, especially when seeking inhibitors of enzymes where the assays are not suitable for high throughput screening. A large percentage of enzyme targets have metal ions, such as Mg^{2+}, Ca^{2+}, and Zn^{2+}, in their active sites that play an important role in substrate binding and catalysis.[13,14] Docking compounds into such metal-containing active sites is very challenging because of the multiple coordination geometries and the lack of sufficiently accurate force field parameters for the ligand-metal interactions.[15] Their presence may alter the hydration and the protonation state of residues, such as Asp, Glu, Arg, Lys, and His in the active site, both factors that are difficult to determine directly from crystal structures. Metal ions seen in crystal structures, directly bound to side chains of the target protein, can be accounted for during docking. Optimizing metal ion parameters such as the radius, partial charge, and well depth can enhance the accuracy of docking.[16–18]

In addition to those bound by the target proteins, many compounds of interest directly bind metals present in the biological environment. Magnesium and manganese bind avidly to phosphates and carboxyls; Mg^{2+} will generally coordinate at least one water molecule. Transition metals such as zinc and iron can form partially covalent bonds with imidazole nitrogens, amines, guanidiniums, and sulfurs.[19] Even when we can locate metal ions that are bound only to the substrate, as in co-crystal structures of enzymes, these metals cannot be incorporated directly into the grid, and are thus not present during the docking.

One way to account for possible direct metal ion binding would be to alter the protonation state of compounds before docking.[20–22] We explored this approach in screen-

The Supplementary Material referred to in this article can be found at http://www.interscience.wiley.com/jpages/0887-3585/suppmat/

Grant sponsor: NIH; Grant number: 5UO1-AI053858-03; Grant sponsor: US Army; Grant number: DAMD17-02-1-0699; Grant sponsor: Mission Pharmacal Company, San Antonio, TX.

*Correspondence to: Catherine H. Schein, PhD, Departments of Biochemistry and Molecular Biology/Microbiology and Immunology, University of Texas Medical Branch, 301 University Blvd., Galveston, TX 77555-0857. E-mail: chschein@utmb.edu

Received 22 May 2006; Revised 4 August 2006; Accepted 8 September 2006

Published online 20 February 2007 in Wiley InterScience (www.interscience.wiley.com). DOI: 10.1002/prot.21249

ing libraries for inhibitors of adenylyl cyclase toxins (AC-toxins), enzymes produced by many pathogenic bacteria, which catalyze the intracellular production of cAMP from ATP.[23–26] These include Edema Factor (EF), an extracellular Ca^{2+}/calmodulin-dependent toxin produced by *Bacillus anthracis*,[27,28] and CyaA of *Bordetella pertussis* (which causes whooping cough).[29–31] Recent crystal structures of EF and CyaA, complexed with substrate analogues and small molecule inhibitors, offer detailed views of the active site residues and metal ions that are essential for catalysis.[27,28,32–34] While the first co-crystal structure of EF[27] (PDB structure 1K90; Fig. 1) showed a single Yb^{3+} ion in the active site, a second structure done in the presence of the more biologically relevant metal, Mg^{2+}, showed two ions, one coordinated by protein side chains and water, and the other bound only to the phosphates of the ATP substrate analogue[28] (PDB structure 1XFV; Fig. 1). To further complicate the issue, a recent structure of the *B. pertussis* CyaA toxin (PDB structure 1ZOT; Fig. 1) has three Mg^{2+} ions in the active site, two of which have ligands to both the protein and the bound substrate analogue (EMA), and one that has ionic bonds only to the phosphate backbone of EMA (Figs. 1 and 2). None of these active site metal configurations matches that of mammalian adenylate cyclase, which has a typical two-metal ion binding site,[35,36] with both metals tightly coordinated by anionic groups on the protein and the substrate.[37]

Thus, while all three AC toxins had a metal ion in the same position, the two done in the presence of Mg^{2+} had at least one additional metal that could not be included in the docking grid. Here, we analyzed how the additional metals affected the docking accuracy and how best to compensate for them during library screening. First, we compared the performance of three programs, AutoDock, LigandFit/Cerius2, and FlexX, in docking substrates and inhibitors to the three EF and CyaA active sites, with that of the mammalian AC serving as control. While all three programs have been shown to be useful for various projects, it is not clear which is best suited for docking proteins with metal ions in their active sites. We assessed docking accuracy by comparing the docked positions of ATP analogues (3′-dATP or 2′3′-ddATP) in the active sites of EF and CyaA with those determined experimentally by X-ray crystallography. We determined (1) which docking programs were most accurate in placing the substrate in the active site and (2) how the accuracy of the docking was related to the protonation state of the docked ligand. We found that accuracy was lower for all programs when docking into the sites that contained metals coordinated primarily to the ligands, and could be improved by appropriate protonation of the phosphates of ATP analogues. We then tested the effect of different protonation states on how a series of test compounds, previously selected from compound libraries, was ranked energetically. The AutoDock ranking order was relatively impervious to the protonation state of the ligand, while that of FlexX showed significant differences. This data shows that, depending on docking program and receptor site, alternate protonation states of ligands should be considered during library screening.

MATERIALS AND METHODS

Ligands and Protein

Protein structures and active site regions

Two crystal structures of edema factor (EF) complexed with calmodulin and a non-cyclizable nucleotide analog, 3′-deoxy-ATP (3′-dATP) were used, that differed in the metal ion(s) used for the crystallization. These were PDB file 1K90, resolution 2.75 Å, *R*-value 0.225; where one Yb^{3+}coordinates carboxyl groups from residues Asp491 (Yb-O distance: 2.14 Å, 2.56 Å), Asp493 (2.16 Å, 2.23 Å), and His577 (Yb-N: 2.78 Å) and an oxygen atom from the α-phosphate group of 3′-dATP(Yb-O: 2.38 Å); and PDB file 1XFV,[28] resolution 3.35 Å and *R*-value 0.263, with two Mg^{2+} ions, which are about 4.32 Å away from each other in the catalytic site. The first coordinates in a fashion similar to the single metal in 1K90. The second Mg^{2+} coordinates only with 3′dATP phosphates and does not interact directly with the protein. The second ion was not included in the docking grid.

The structure of CyaA of *Bordetella pertussis* was taken from PDB file 1ZOT (resolution 2.20 Å and *R*-value 0.252) of a complex with the nucleotide analog inhibitor adenine-9-yl-ethoxymethyl-hydroxyphosphinyl-diphosphate (EMA). Residues in the active site of EF, Asp491, Asp493, Arg329, Lys346, Lys353, Lys372, Ser354, Thr548, His577, Thr579, and Asn583, align with residues Asp188, Asp190, Arg41, Lys58, Lys65, Lys84, Ser66, Val27, His298, Thr300, and Asn304, respectively, of CyaA. Of the three Mg^{2+} in the active site, two have bonds to protein side chains (and are thus in the docking grid) and EMA, and one is only on the inhibitor (and is thus not represented). While one Mg^{2+} interacts with carboxyl groups from residues Asp190 and Asp188, and the α-phosphate of EMA, the other Mg^{2+} ions have rather different coordination (Fig. 1) from that seen in EF.

The structure of mammalian adenylate cyclase was taken from PDB files 1CJV[37] resolution 3.00 Å and *R*-value 0.203, which shows a complex of the catalytic domains of mammalian adenylyl cyclase with β-L-2′,3′-dideoxyATP (2′3′-ddATP) There are two metal ions (Zn^{2+} and Mg^{2+}), "bridged" by carboxyl groups of Asp396 and Asp440, which allows them to remain close (3.68 Å) to one another. The Mg^{2+} forms coordinate bonds with the oxygen atoms from the three phosphate of 2′3′-ddATP, while the Zn^{2+} coordinates the α-phosphate. Both metals were used for calculation of the docking grid.

Ligands

3d′ATP, 2′3′ddATP, and EMA (Fig. 2) are noncyclizable nucleotide analogues of ATP. PGE_2-imidazole is a covalent adduct[38] that inhibits the accumulation of cAMP in cells treated with EF or CyaA. The other compounds in Figure 7 were chosen first by a pharmacophore screening of the NCI and ZINC databases, and then ranked according to their AutoDock and ChemScore functions, as will be described separately (Chen et al., in preparation). All carboxyl groups and phosphate groups were deprotonated or protonated as specified for tests. For all the dockings

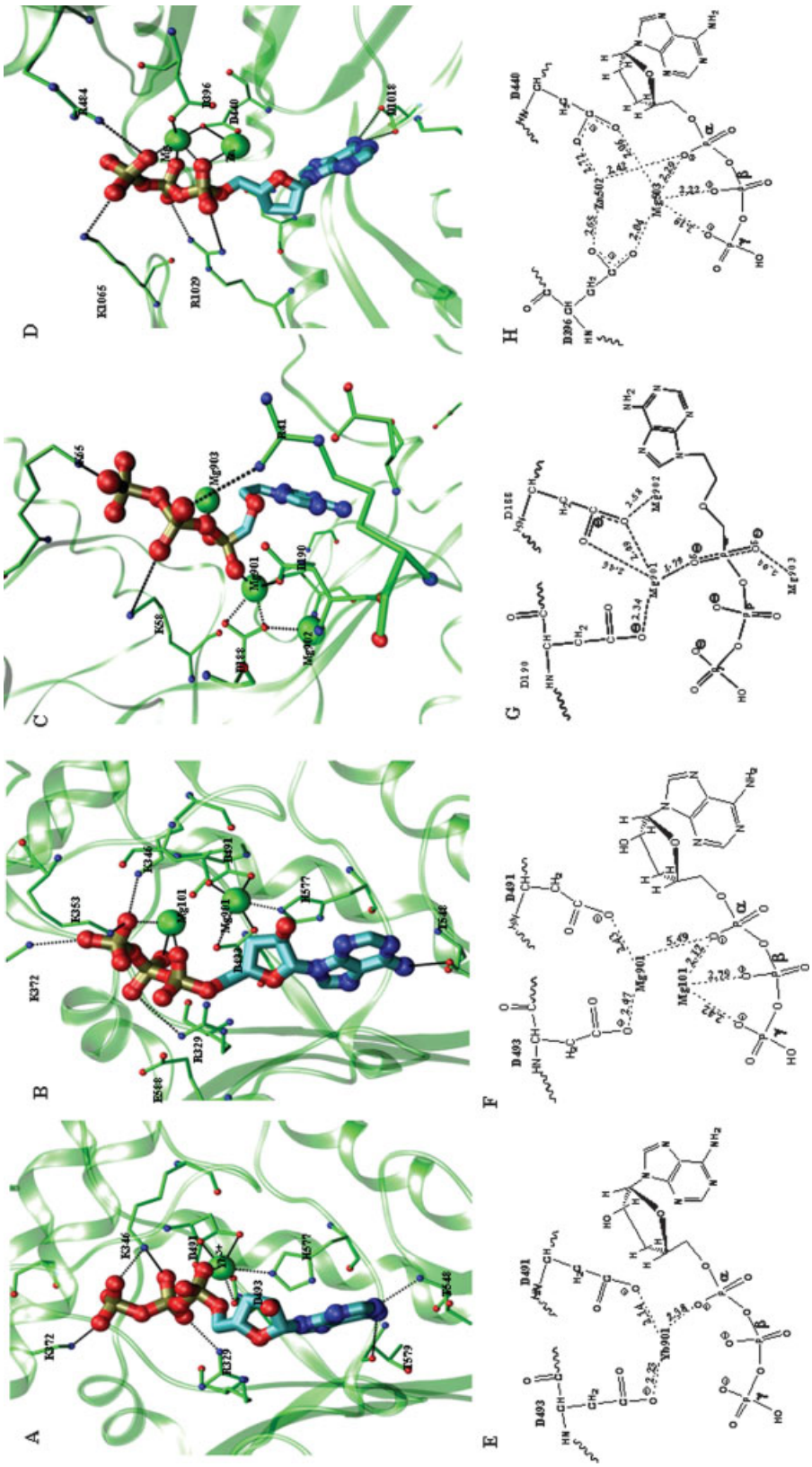

Fig. 1. Comparison of the metal sites in crystal structures of *B. anthracis* anthrax EF (1K90, **A**,**E**: 1XFV, **B**,**F**), *B. Pertussis* Cya (1ZOT, **C**,**G**) and mammalian AC (1CJV, **D**,**H**). The bottom figures show the metal ion coordination schematically. A and E: the active site of EF (from 1K90) with one Yb^{3+}. Residues Asp491, Asp493, His577 of EF and the α-phosphate of 3′-dATP chelate the metal ion. B and F: The active site of EF (from 1XFV) which shows two Mg^{2+} ions 4.32 Å apart. The Mg901 is chelated by residues Asp491, Asp493, and His577 of EF, while Mg101 is chelated by the oxygen atoms from the three phosphates of 3′-dATP. C and G: the active site of CyaA (from 1ZOT) which shows three Mg^{2+} ions. Mg902 interacts with Asp188. Mg902 interacts with the α-phosphate of EMA. Mg901 is chelated by residues Asp188, Asp190, and the α-phosphate EMA. D and H) the active site of mammalian adenylate cyclase(from 1CJV) with two metal (Zn^{2+} and Mg^{2+}) ions, 3.7 Å apart. Both metals are bridged by the carboxyls of Asp396 and Asp440 from the protein; the Mg^{2+} ion is chelated by α, β, γ phosphates of 2′3′-ddATP and the Zn^{2+} ion by the α-phosphates of 2′3′-ddATP.

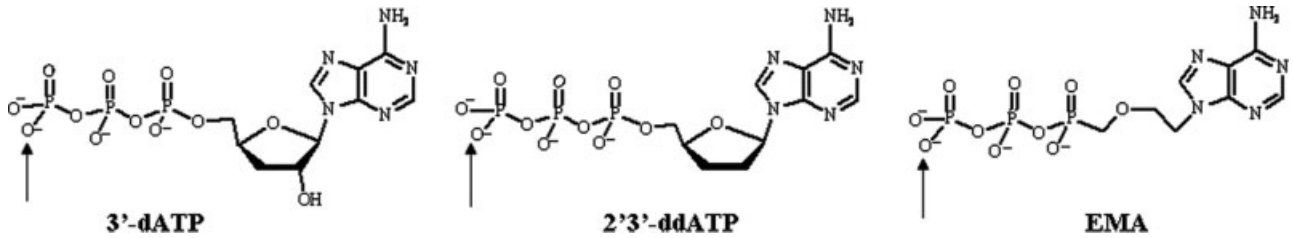

Fig. 2. Structures of 3′-dATP, 2′3′-ddATP, and EMA, the ligands used in this study. Arrows indicate where hydrogens were added to test the effect of partial protonation on docking position.

of 1K90, Yb^{3+} was replaced with the more physiological Mg^{2+} at the same position, which allowed better comparison of the energy data. Tests done with Autodock and different metal ions and charges indicated that there was relatively little difference in the scoring or ranking of ligands (data not shown).

Docking Programs and Scoring

AutoDock (version 3.0.5)[1,2] (http://www.scripps.edu/mb/olson/doc/autodock), has three different algorithms for docking: simulated annealing (SA), genetic algorithm (GA), and "`" (LGA). The LGA was chosen for these studies as our own results and those of others[2,39] indicated this is a most efficient and robust algorithm. Docked conformations are rated by a scoring function that includes terms for van der Waals, hydrogen bond, and electrostatic interactions, plus internal energy of the ligand. The iterations were set to 200[1] and population size 100. The ligand and solvent molecules were removed from the crystal structure to obtain the docking grid and the active site was defined using AutoGrid. The grid size was set to 90 × 90 × 90 points with grid spacing of 0.375 Å. The grid box was centered on the center of the ligand from the corresponding crystal structure complexes. For the Zn^{2+} ion in 1CJV, parameters were set as described in Refs. 16 and 17: radius 0.87 Å, well depth 0.35 kcal/mol, and charge +0.95e. The Mg^{2+} ions used Amber force field potentials as defined in the AutoDock program. The absolute, but not the relative docking energies, were altered by the charge assigned to the magnesium (supplementary data). We assigned a partial charge of +0.8 as we found that if the formal charge was set to +1.2, the interaction of the ligand and the carboxyl group of the ligand was overestimated and led to very short oxygen-Mg distances. The conformation with the lowest binding energy was used to analyze ligand placement.

LigandFit/Cerius2(version 4.10)[3] uses a Monte Carlo conformation search procedure to generate many ligand conformations for docking. A ligand/shape comparison algorithm is used to generate ligand conformations consistent with the shape of the docking site(s) on the protein. The substrates or inhibitors from the PDB file are used to define the active site. The grid points within the default distance of the substrates or inhibitors that are unoccupied by the receptor atoms were defined as the active site. The maximum conformations saved were set to 100. The energy grid was set up using the Piecewise linear potential (PLP) v.1. The poses were evaluated by PLP-DockScore.

FlexX,[4–7,9,40] as included in Sybyl7.0, uses an incremental construction algorithm, where the ligand is decomposed at rotatable bonds into discrete fragments. Then a base fragment is chosen and placed by using a technique called pose clustering.[40] The other parts of the ligand are then added in such a way as to maximize interactions. Default docking settings were used, except that the number of conformations was set to 100. Formal charges of the metals were assigned by the SYBYL program. For FlexX docking, the best ranked pose was selected from the ChemScore.

RMSD (root mean square deviation) between the heavy atoms of the substrate analog positions in the crystal structures with the docked conformations were determined with MolMol[41] using the "CalcRmsd" command.

Cell Culture

Murine monocyte/macrophage cells (RAW 264.7) were propagated in T75 flasks containing Dulbecco's Modified Eagle's Medium (DMEM) (Mediatech, Herndon, VA) at 37°C with 5% CO_2. The culture media contained 10% fetal bovine serum (FBS), 100 μg/mL penicillin/streptomycin, and L-glutamine.

Cell Assay for Edema Factor Activity

Cells were plated 1×10^6 cells per well in DMEM containing 10% FBS, 100 μg/mL penicillin/streptomycin, and L-glutamine with isobutylmethylxanthine (IBMX) (50 μ*M*) IBMX in 48 well tissue culture plates and allowed to adhere overnight at 37°C in 5% CO_2. PGE_2-imidazole, Protective Antigen (2.5 μg/mL PA), and EF (0.625 μg/mL) are diluted with assay media containing DMEM (without phenol red) with 100 μg/mL penicillin/streptomycin and L-glutamine. Media is aspirated from the cells and replaced with varying concentrations of the inhibitors or PGE_2 imidazole (100, 10, 1 and 0.1 μ*M*) with PA and EF and is incubated for 4 h at 37°C in 5% CO_2 for 4 h. Following the incubation period, the culture supernatants were removed (extracellular cAMP) and transferred to a new 48 well plate for cAMP determination.

[1]Our data indicate that 60 iterations is sufficient for compound ranking in library screening but not for achieving the lowest binding energies.

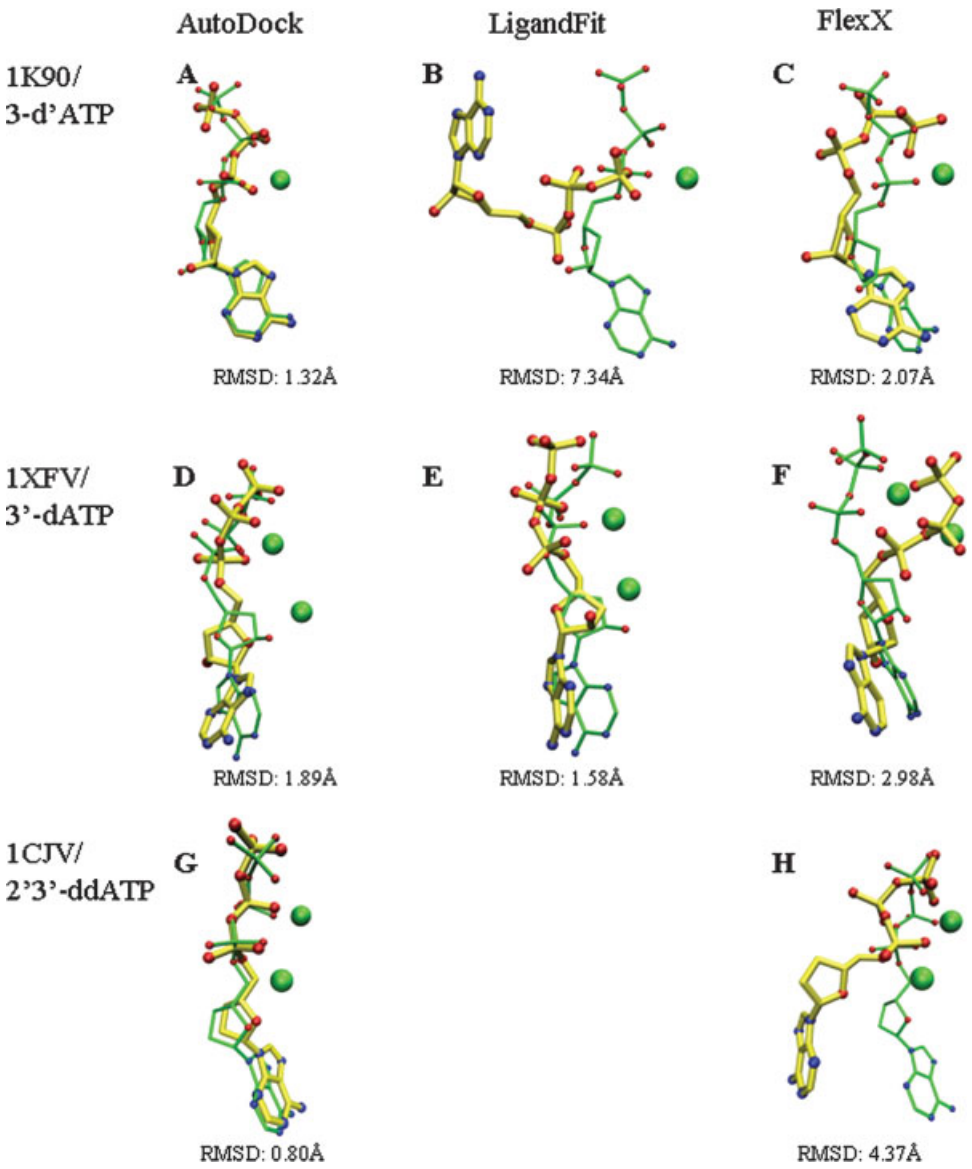

Fig. 3. Comparison of how closely the poses of substrate analogues (yellow, thick lines) determined by three docking programs matched the experimentally determined position (green, thinner lines) in co-crystal structures of Anthrax EF (1K90, one metal, and 1XFV, two metals) and mammalian AC (1CJV). [Color figure can be viewed in the online issue, which is available at www.interscience.wiley.com.]

cAMP Determination

The extracellular cAMP concentration in the supernatants was measured with a cAMP-specific ELISA from Assay Designs, (Ann Arbor, Michigan) per manufacturer directions.

RESULTS

The Three Programs Vary in Accuracy in Posing ATP Analogs into the Active Site of EF

As a first step, we compared how AutoDock, LigandFit/Cerius2 and FlexX docked analogs of ATP into the active sites of EF as represented by two different crystal structures, 1K90 (where one Yb^{3+} atom binds in the active site) and 1XVF (with one Mg^{2+} ion bound to the protein and one coordinated to the phosphates of 3′-dATP). Based on the RMSD of the posed substrate analogues relative to that in the crystal structures (Fig. 3), the best ranked poses from AutoDock were quite close to the experimentally determined position in both crystal structures of EF and that of mammalian AC. However, the other two programs showed more variation in their abilities to correctly position the ligands. In general, the lowest energy conformation did not exactly match the conformation with the lowest RMSD to the experimental position (Table I), but with few exceptions the two conformations did not differ significantly.

TABLE I. Heavy Atom RMSDs (See Fig. 3) Between the Docked Conformations of Substrate Analogues From Three Programs and the Positions in the Crystal Structures and the Corresponding Docking Scores

	1K90 RMSD/score	1XFV RMSD/score	1CJV RMSD/score
AutoDock			
Lowest RMSD*	0.91 Å/−16.2	1.61 Å/−12.3	0.75 Å/−12.6
Lowest energy**	1.32 Å/−16.9	1.89 Å/−13.6	0.80 Å/−13.5
LigandFit			
Lowest RMSD*	1.43 Å/−115.01	1.34 Å/−109.59	Not done
Lowest energy**	7.30 Å/−121.42	1.58 Å/−110.40	Not done
FlexX			
Lowest RMSD*	1.69 Å/−41.53	2.49 Å/−40.10	3.79 Å/−49.93
Lowest energy**	2.07 Å/−42.64	2.98 Å/−43.96	4.37 Å/−60.54

*The docked conformation is selected for the best fitted pose with the lowest RMSD value.
**The docked conformation is selected for the best ranked pose with the best calculated score.

TABLE II. Difference in Selected Distances Between Non-Ethereal Phosphate Oxygen Atoms of the Substrate Analogues in the Best Ranked Pose and Those of Side Chains in EF in the Co-Crystal Structures 1K90 and 1XFV or for Mammalian Adenylyl Cyclase Co-Crystal Structure 1CJV

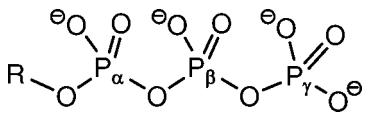

	3′dATP	Metal[a]	Arg329	Lys346	Lys353	Lys372
AutoDock						
1K90	α PO_4	0.61		0.51	[b]	
	β PO_4	0.18	0.80	0.21		
	γ PO_4			0.09	[c]	0.67
1XFV	α PO_4	0.28	0.52			
	β PO_4	[c]	[b]	[c]	0.70	
	γ PO_4	0.97		0.29	0.37	0.32
LigandFit/Cerius2						
1K90	α PO_4	[b]		[b]	[b]	
	β PO_4	[b]	[b]	[b]	[c]	
	γ PO_4	[c]		0.07		[b]
1XFV	α PO_4	0.73	[b]			
	β PO_4	[c]	0.92			
	γ PO_4	0.09		0.01	0.34	0.45
FlexX						
1K90	α PO_4	0.10	[c]	1.62	[b]	
	β PO_4	[b]	[b]	0.36		[c]
	γ PO_4		[c]	[b]	[b]	1.03
1XFV	α PO_4	0.17		[b]		
	β PO_4	[c]	[b]			
	γ PO_4	0.19	[b]	0.36	[b]	[b]
	2′3′ddATP	Mg^{2+}	Zn^{2+}	Arg484	Arg1029	Lys1065
AutoDock						
1CJV	α PO_4	0.34	0.05		[b]	
	β PO_4	0.30			0.26	
	γ PO_4	1.13		0.03		0.17
FlexX						
1CJV	α PO_4	0.49	0.20		[b]	
	β PO_4	[b]			0.35	[c]
	γ PO_4	2.38		0.10		[b]

*A "Blank" entry implies that the specified distance was greater than 3.60 Å in both the crystal structure and the docked conformation. All reported distances are in Å.
[a]For 1K90, Yb^{3+} was converted to a Mg^{2+}; or 1XFV, only MG101 was used (Fig. 1).
[b]This distance is within Hydrogen or coordination bond length (distance <3.60 Å) in the crystal structure but not in the docked conformation.
[c]This distance is not within hydrogen or coordination bond length in the crystal structure (distance >3.60 Å), but it is in the docked conformation.

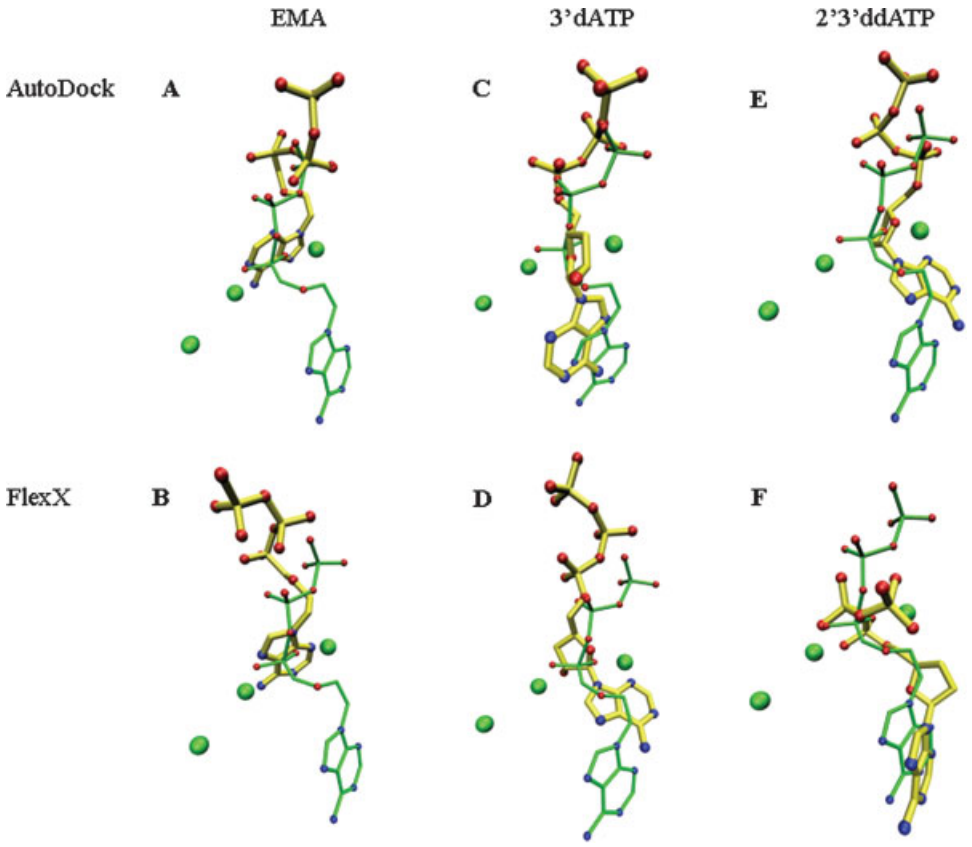

Fig. 4. Comparison of how closely the poses of the inhibitor EMA and two other ATP analogues (yellow, thick lines) determined by AutoDock and FlexX matched the experimentally determined position (green, thinner lines) of EMA in the active site of CyaA (from PDB file 1ZOT). [Color figure can be viewed in the online issue, which is available at www.interscience.wiley.com.]

The phosphate groups from the best ranked poses of all three programs are near the metal ion and interact with positively charged residues (Arg329, Lys353, and Lys372), consistent with the crystal structures. However, the distances between the interacting atoms and positions of the phosphates differ considerably (Table II). The individual interactions from AutoDock are quite similar to the interactions from the experimental structure. AutoDock also performed best for docking 2′3′-ddATP into the mammalian adenylate cyclase (1CJV) active site [Fig. 3(G,H)] with an RMSD value of 0.80 Å. The interactions of the phosphate groups with the metal ions and the positively charged residues are listed in Table II. The FlexX lowest energy conformation for the adenine ring is particularly far from that seen in the crystal structure.

Docking ATP Analogues into the Active Site of CyaA is Altered by Protonation

In contrast, neither AutoDock nor FlexX could correctly position the adenine ring of EMA in the active site of Cya A (Fig. 4), where only two of the three Mg^{2+} ions were included in the protein grid. However, AutoDock placed another ATP analogue, dATP, close to the EMA position, and FlexX superposed the 2′3′-ddATP at the EMA position. Thus, the ability of the programs to match the crystal structure position was dependent on the ligand.

There is a pKa for the phosphates of ATP and analogues thereof at about pH 6.5, and the phosphate oxygens at pH's above this are considered to be deprotonated.[42] However, analysis of the interactions of EMA with residues in the active site of CyaA indicated its γ-phosphate group might be protonated, as the binding of the third Mg^{2+} would be expected to render this group as much as two log values more acidic.[42,43] The binding environment of the ATP analogues in the active sites of the three AC-toxins is shown in detail in Figure 5 and Table III. Figure 5(D) shows one possible coordination network for the third Mg^{2+} in the CyaA crystal structure that could serve to stabilize and neutralize the bound triphosphate moiety of EMA. Magnesium ions are typically coordinated to six groups in an octahedral geometry, and in a hydrated active site at least one of these ligands will be water. The distances of the γ-phosphate and the Mg903 to the carboxyl-oxygens of Glu308, both about 4.6 Å [Fig. 5(C)], suggest that two water molecules could serve as bridges between this side chain and the bound EMA.

This model would suggest that the γ-phosphate group of EMA is protonated in the bound state (or behaves as if it were protonated due to the presence of the metal ion).

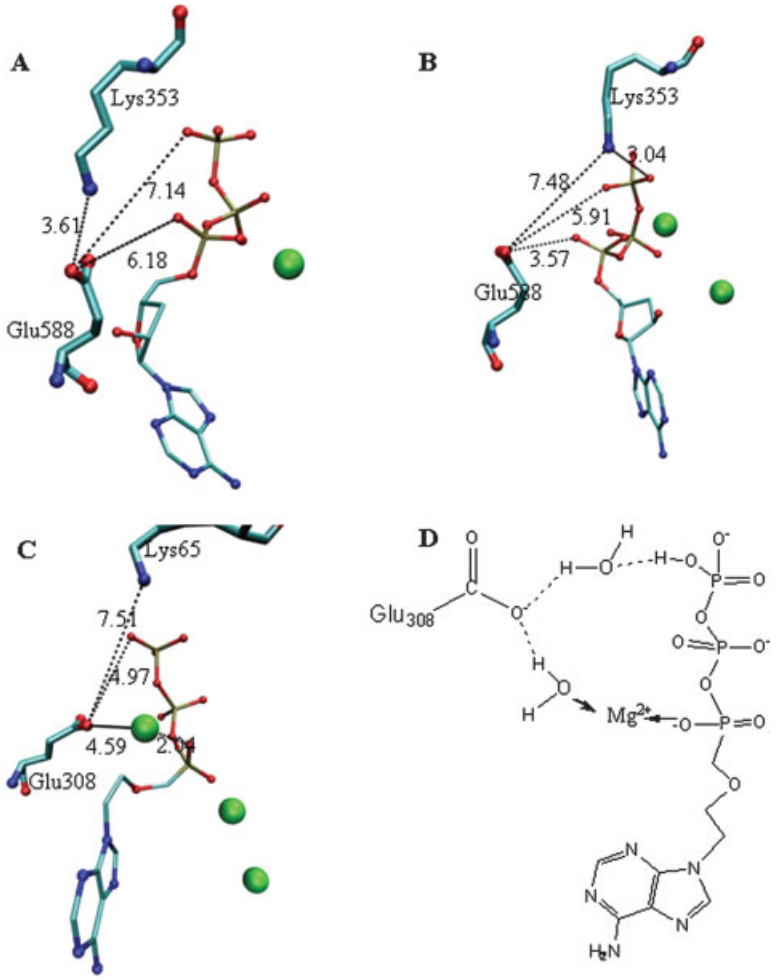

Fig. 5. The metal ion type affects the relative position of the ligand and the residues in the active site of EF (**A**, 1K90, 1 Yb^{3+}; **B**, 1XFV, 2 Mg^{2+}) and CyaA (**C** and **D**, 1ZOT, 3 Mg^{2+}). In particular, a pair of conserved, charged residues (Glu588,Lys353 in EF and Glu308,Lys65 in CyaA) form a salt bridge in the 1K90 structure of EF that contains Yb^{3+}(A) but not in either of toxin structures that contain ligand-bound Mg^{2+} ions (B,C). (D) Proposed coordination network for Mg^{2+}903, near the α-phosphate oxygen, in 1ZOT, that includes the implied protonation of the γ-phosphate. [Color figure can be viewed in the online issue, which is available at www.interscience.wiley.com.]

Therefore, we tested the effects of protonation at the γ-phosphate on the docking accuracy of EMA and the other ATP analogues (Fig. 2). As Figure 6 shows, adding a proton to 3′-dATP or 2′3′-ddATP reduced the accuracy of docking into EF (1K90, 1XFV) or into the "true" two metal site of the mammalian protein (1CJV) [Fig. 6(A–F)]. On the other hand, the partially protonated EMA was accurately docked by both AutoDock and FlexX into a position close to that seen in the crystal structure of CyaA. Thus docking accuracy depended on the active site and the effective charge on the ligand.

Effects of Protonation of Carboxyls on Ranking Compound Libraries

The results with the EMA docking indicated that protonation state may improve docking accuracy, at least when using ATP analogues, and may serve as a way to account for ligand-bound metals. However, when we compared the energies for docking EMA into the active site of 1ZOT, the binding energy for the protonated form was actually slightly higher (less favorable) than that for the unprotonated form. This was consistent with the data in Table I, where the lowest energy conformation was generally not the one with the lowest RMSD to the crystal structure conformation. Thus the energy values were not completely consistent with docking accuracy. This was important, as particularly when screening large libraries, alterations in ranking according to docking scores will determine whether a compound is tested or ignored. We thus determined the effect of protonating potential metal binding sites (carboxyl groups) on the docking scores based ranking of a set of compounds that had been previously selected from the NCI and ZINC databases.

TABLE III. Corresponding Residues Between EF and CyaA and Their Interactions With Metal Cations and ATP Analogues in the Two EF Structures (1K90, 1XFV) and That of CyaA (1ZOT)

Structure	Interaction pair		Interaction pair		Interaction pair	
1K90	Asp491	Metal	Asp493	Metal	His577	Metal
1XFV	Asp491	MG901	Asp493	MG901	His577	[a]
1ZOT	Asp188	MG901	Asp190	MG901	His298	MG901
1K90	Lys346	α,β,γ-PO_4	Arg329	β-PO_4	Lys353	[b]
1XFV	Lys346	β-PO_4	Arg329	β-PO_4	Lys353	γ-PO_4
1ZOT	Lys58	β-PO_4	Arg41	β-PO_4	Lys65	γ-PO_4
1K90	Lys372	γ-PO_4	Thr579 (carbonyl)	Adenine-N6	Thr548 (carbonyl)	Adenine-N6
1XFV	Lys372	γ-PO_4	Thr579 (carbonyl)	Adenine-N6	Thr548 (carbonyl)	Adenine-N6
1ZOT	Lys84	[c]	Thr300 (carbonyl)	Adenine-N6	Val271 (bb-C=O)	Adenine-N6

The interaction between Ser354 and the γ-PO_4 in 1K90 is not seen in 1XFV, nor does the equivalent Ser66 in 1ZOT show this bond.
[a]His577 is close to the metal, but not correctly oriented to constructively interact. This is consistent with other reports that Mg^{2+} ions have (statistically) a low probability of being coordinated by His-imidazoles in proteins.[44]
[b]The distances between Lys353 and the α- and γ-phosphate oxygens are >3.6 Å.
[c]The distance between Lys84 and the γ-phosphate oxygens are >3.6 Å.

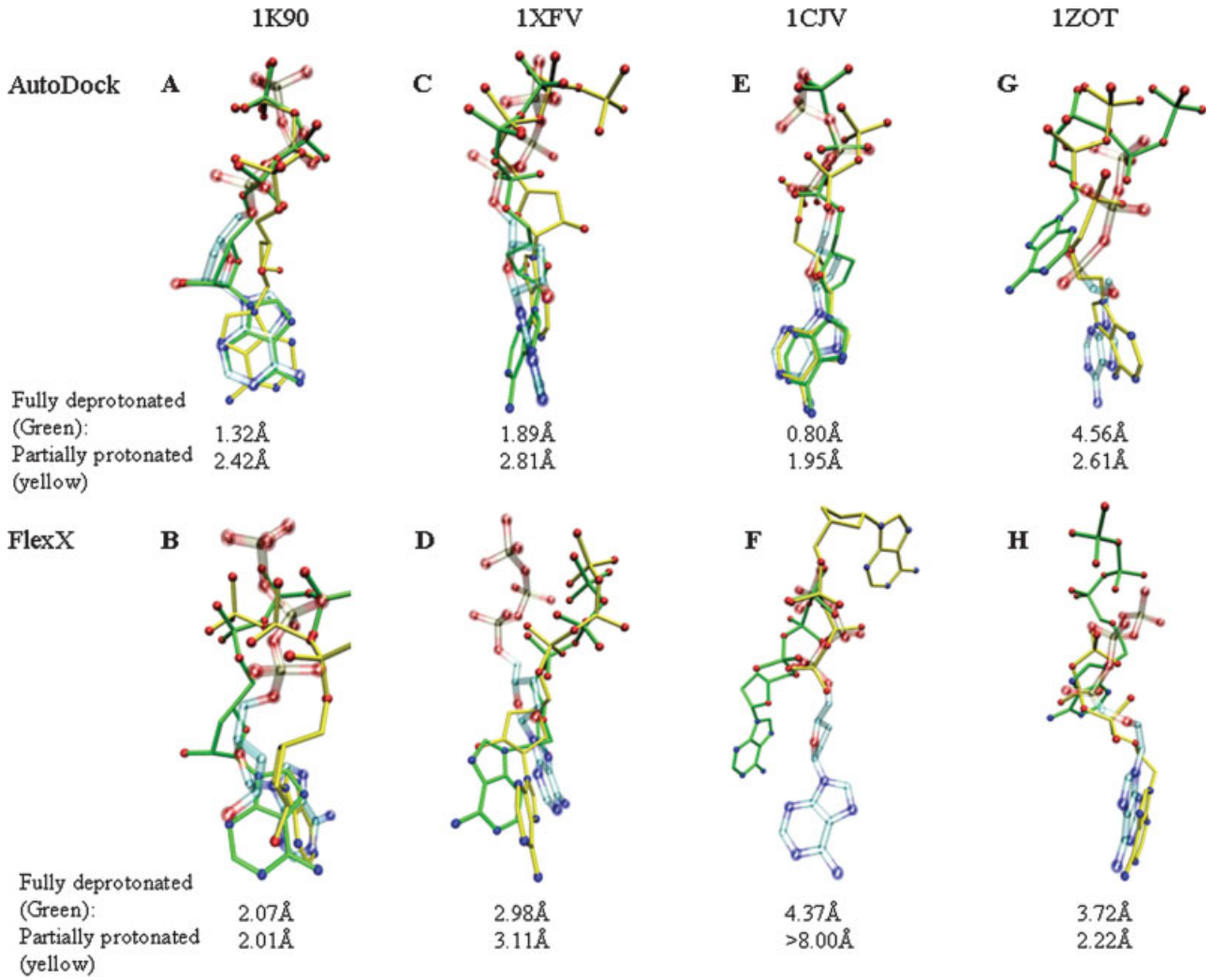

Fig. 6. The protonation states of ATP analogues 3′-dATP (**A**–**D**), 2′3′-ddATP (**E**,**F**), and EMA (**G**,**H**) affect the ability of AutoDock and FlexX to match the experimentally determined position when docking into EF (1K90, A,B; 1XFV, C,D), Cya A (1ZOT, E,F) and mammalian AC (1CJV, G,H). The deprotonated analogues (green, thinner lines) docked closer to the crystal structure position (lowest RMSD value, given below each figure) than the partially protonated ones (yellow, thicker lines), except for the CyaA active site (G,H). The crystal structure conformations for each analogue are shown in blue for comparison.

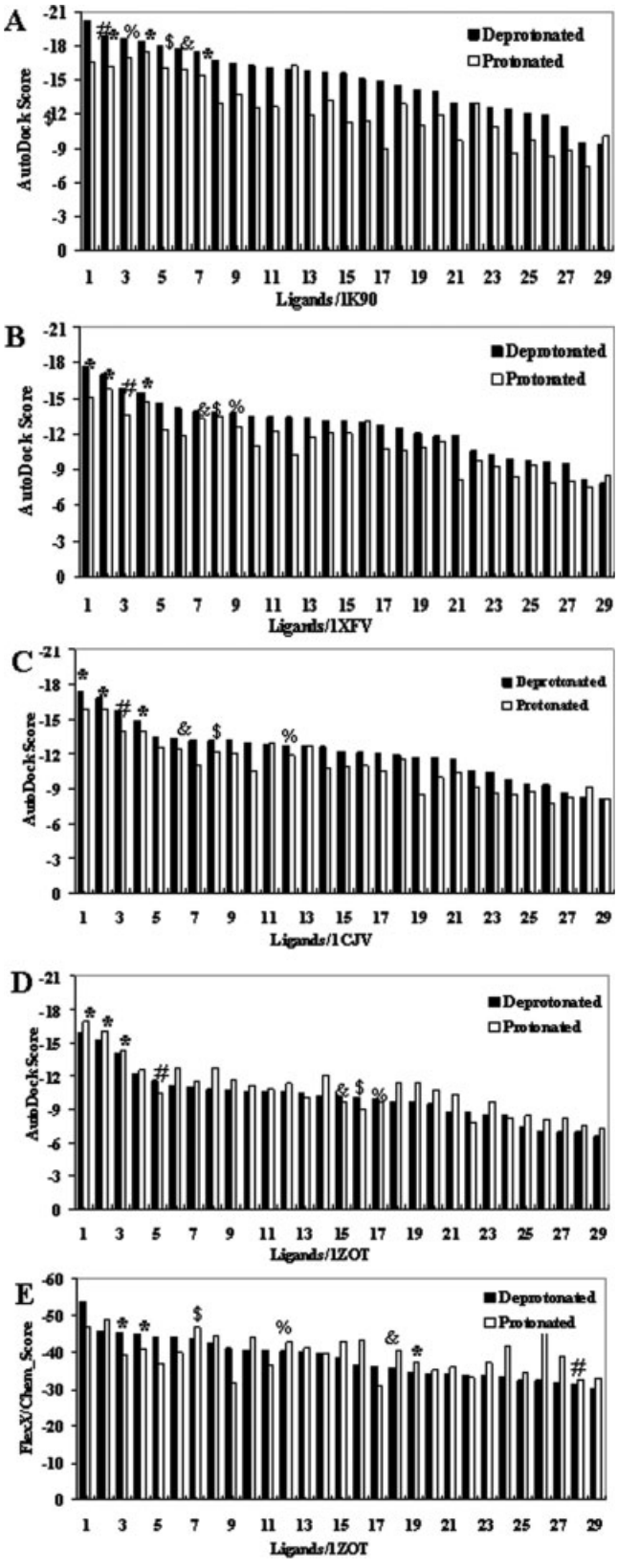

Protonating the compounds had relatively little effect on the ranking with the AutoDock program, for both crystal structures of EF (i.e., for the active sites that originally contained one Yb^{3+} or two Mg^{2+}) or mammalian AC [Fig. 7(A-C)]. Of 29 compounds, only three showed a radically different ranking when protonated. As Figure 7 also indicates, ranking of the deprotonated ligands by AutoDock was generally a good indication of their ability to inhibit EF, in a cell assay that will be described in more detail separately (Chen et al., in preparation).

The results with docking into the active site of CyaA were quite different [Fig. 7(D,E)]. The AutoDock scores were overall lower (more favorable) for the protonated compounds but, as seen for the EF active site, there were only a few changes in overall compound ranking. The FlexX docking results showed a much more drastic alteration with protonation state. Of the 29 compounds, 11 changed rank considerably, and several of the inhibitors that had previously been ranked in the 10 best were now close to the bottom of the list. We analyzed the dockings of several of the compounds whose rank order was greatly affected by protonation. Protonation of the carboxyl group(s) on large aromatic side chains completely abrogated their interaction with the active site metal ion (data not shown). This caused a repositioning of the large side chain, such that it moved from the active site pocket to a less energetically favorable position. This effect may be due to FlexX's decomposition of compound ligands into separate entities, or to other internal details of how the program handles charges during the docking.

DISCUSSION

In this work, we specifically looked at how to account for the effects of "missing" metal ions, those bound directly to the substrate or inhibitor, when using docking programs. High resolution structures of metalloenzymes that have optimal activity with Mg^{2+} are often based on crystals that use metal ions with a higher molecular mass, which are easier to visualize in electron density maps. While larger metals, such as Yb^{3+} or Mn^{2+}, may support activity,[28,45] their presence can distort the active site, and in some cases alter the fidelity of the reaction.[46,47] For example, the crystal structure of the EF active site in the presence of the lanthanide Yb^{3+} contained only one metal ion, while a subsequent co-crystal structure done in the presence of Mg^{2+} contained two (Fig. 1). A crystal structure of the closely related toxin CyaA contained three

Fig. 7. Comparison of the docking scores for the deprotonated (solid bars) and carboxyl-protonated (open bars) forms of 25 compounds selected from the NCI and ZINC databases, as well as γ-phosphate protonated/deprotonated ATP(%) and three analogues (#: the CyaA inhibitor EMA; &: 3′-dATP; $: 2′3′-ddATP) thereof. The selected compounds and the ATP analogues were ranked according to their deprotonated docking scores in order of increasing energy. The three compounds that significantly inhibited ($IC_{50} < 50$ μM) in the EF assay of the 25 selected are indicated by *. (**A**–**D**) the compounds docked into 1K90, 1XFV, 1CJV, and 1ZOT with AutoDock. (**E**): the compounds docked into 1ZOT with FlexX.

Mg^{2+} ions in a similar active site. At least one additional Mg^{2+} ion in both of the toxin active sites was coordinated exclusively to the phosphates of the bound substrate. The results shown in this paper indicate that this direct binding of metal ions to charged ligands affects the docking accuracy of ATP analogues (Figs. 3 and 4). Specifically, protonation at the γ-phosphate position (Fig. 5) improved the accuracy of docking in one instance where direct Mg^{2+} binding was observed (Fig. 6). Further, depending on the program used, protonation of selected compounds could reduce the docking energies and alter the ranking of selected compounds (Fig. 7). The latter point is particularly important, as docking scores are often used to select compounds from large libraries for further assay.

Below, we discuss these results in more detail, with respect to specific changes in the active site related to the metal ion used to obtain the structure, and how the results from the programs we tested were affected by protonation of ligands before docking.

Metal Ion Choice Affects the Active Site

One would anticipate that the metal ion choice during crystal preparation would affect the position and effective charge (protonation state) of residues in the active site, as coordination geometries vary greatly. For example, the divalent cations Mg^{2+}, Ni^{2+}, and Co^{2+} form predominantly octahedral complexes, while Zn^{2+} prefers tetrahedral and Cu^{2+} square planar geometries.[48,49] Profound differences are also seen in the coordinating amino acids in crystal structures. For example, Mn^{2+} has similar binding sites to Mg^{2+}, but differs in having fewer coordination bonds to Ser/Thr-OH groups and many more to His-imidazoles.[44] Further, physiologically relevant metal ions such as Mg^{2+} can be coordinated by water atoms and oxygen atoms of the substrate, as well as protein side chains.[35] While our two active sites for EF look superficially similar (Fig. 1), there are obvious differences in the proximity of charged side chains (Fig. 5; Table III). The metal ion Yb^{3+} in the EF structure 1K90 is coordinated by the carboxyls of Asp491 and Asp493, and the α-phosphate-oxygen of the ATP analogue. It is electronically neutral and does not bond with Glu588, which forms a salt bridge to Lys353. However, when Mg^{2+} is present, the Glu588 (Glu308 in CyaA) carboxyl is much further from Lys353 (Lys65 in CyaA) but closer to the phosphates of the substrate analogues.

While we can clearly see this alteration in charged groups, there are probably additional, more subtle changes that have occurred in these active sites, due to the presence of the ligand-bound metals. In Figure 5(D), we postulate that the hydrophilic Mg^{2+} may increase the number of water molecules in the active site, and suggest how the metal, near the α-phosphate position, might alter the effective charge on the γ- phosphate, based on other studies.[43] These differences in the active site can account for the docking results shown in Figure 6, where protonation at a site distant from the "missing" Mg^{2+}'s original location greatly improved docking accuracy.

Effect of Protonation on Docking Scores

Crystal structures do not allow one to visualize the protonation state of side chains or bound ligands in the active site, but we can draw conclusions based on the proximity of charged residues in the active site of EF and CyaA [Fig. 5(A–C), Table III]. MD simulations of both EF active sites, with one-Yb^{3+} (1K90) and or 2-Mg^{2+} (1XFV) ions, were unable to distinguish the two in terms of stable binding to the 3′-dATP.[28] Our results are consistent with this, as the docking score rankings of the inhibitors and test compounds were approximately the same for both active sites (Fig. 7). Our docking results indicate that the γ-phosphate group of EMA is partially protonated when it is bound to the CyaA active site (1ZOT), while the γ-phosphate group of 3′-dATP is deprotonated when it is bound to EF, regardless of which metal is used for the co-crystal structure.

However, we consistently saw that the conformation with the lowest docking energy was not the one that best matched the crystal structure position (Table I). We were thus particularly interested in relating protonation of ligands to their rankings, and to how these rankings correlated with their activity in inhibiting EF. Our results indicate that the common practice of deprotonating charged compounds at neutral pH according to their pKa is adequate,[20–22] especially when using AutoDock (Fig. 7). However, when dealing with triphosphate moieties, it is probably wise to test different protonation states, as binding in a biological environment will almost certainly alter their effective charge (Fig. 5). For one of the Mg containing active sites (1ZOT structure of CyaA), protonation led to a docked conformation much closer to that seen in the crystal structures (Fig. 6). However, in the other active sites, protonating the γ-phosphate drove the docked conformer away from the crystal structure position and led to a larger RMSD (Fig. 6).

As shown in Figure 7, the docking scores when the carboxyl groups of the test compounds were protonated were higher (i.e., the binding was less favorable) than when they were deprotonated for three of the four targets. Where the structure indicated the bound ligand would be protonated, as in the CyaA active site, the scores for the protonated forms were lower (more favorable) for most compounds. The average difference in the scores was low, generally less than 1–2 kcal when using AutoDock. Only a few compounds showed large variances, such as number 17 in Figure 7(A), where the score was −14.97 kcal/mol for the deprotonated state and −8.86 kcal/mol for the protonated.

We saw much more variability in the scores and rankings with FlexX [Fig. 7(E)]. We thus do not recommend protonating carboxyl groups of ligands when using AutoDock, but one might test both forms of charged compounds when using FlexX.

Optimizing Parameters to Achieve Better Docking Results

The docking programs we tested have different ways for accounting for the presence of metal ions in the active

site. The interactions between the metal ion and coordinated atoms (including atoms from ligands and from macromolecules) can be considered ionic, covalent,[13] or partially covalent.[18] Some force field parameters for metalloenzymes[16,50,51] and even quantum mechanics based functions[52] have been developed. AutoDock,[1,2] the most reliable program in our studies (Figs. 3 and 7), models the metal-ligand coordination with electrostatics, which may differ from the potentials used by FlexX.[4–8] Neither AutoDock nor FlexX consider the special geometries of the metal-ligand coordinate interaction. We did find that there was an effect of altering the charge on the metal ion on overall docking scores from AutoDock (supplementary material; Methods). We would recommend running similar tests with other metal containing proteins before beginning library screening.

The AutoDock Program Performs Most Reliably

We used two tests for our dockings in this study, similar to those used by others in comparing several programs.[53] The first was how well the programs were able to position substrate analogues into the active site, as compared to crystal structures of the complex. Comparing the position of docked substrate analogues to their experimentally determined position in the crystal structures (Figs. 3 and 4) indicated that the programs varied widely in their reliability, with RMSD values between the docked and experimental conformations of the ligands ranging from 0.8 Å to >8.0 Å. The AutoDock program was most consistently successful in positioning the substrate analogues into both EF structures (1K90, 1XFV) and the mammalian AC (1CJV), and, with protonated EMA, into the CyaA active site. This is consistent with a previous report that AutoDock performed most reliably and robustly in docking of inhibitors to zinc metalloproteinase.[17] The second test was for how well the scoring/ranking by the programs correlated with the inhibitory activity of a group of compounds for which we had assay data. As the position of the starred (inhibitory) compounds on the rank order of Figure 7 shows graphically, AutoDock consistently ranked the active inhibitors and ATP higher than the inactive compounds, while FlexX did not. This would suggest that the electrostatic interaction model of AutoDock is superior for determining the docking mode of inhibitors into proteins that contain metal ions in their active site. The ranking of the compounds by FlexX was not improved by altering protonation, suggesting that there were other problems with the scoring beyond accounting for electrostatic interactions.

In addition, we have seen that the same active compounds also bind equally well to the active site of mammalian adenylate cyclase [Fig. 7(A–C)]. We believe this is due to the fact that both types of active sites are really quite similar in their basic metal binding architecture, as the simplified drawings of the metal binding sites [Fig. 1(E–H)] makes clear. Thus, the active compounds identified in this study by using molecular docking will be further optimized for specificity, before they can be considered adequate therapeutic candidates for alleviating the effects of the bacterial toxins. Studies to this end are currently underway.

CONCLUSIONS

- The use of different metal ions in crystal structures does engender differences in the active site that affect docking accuracy.
- The altered acidity of docked ligands due to direct binding to metal ions may be accounted for by changes in the protonation state.
- The FlexX program scoring function is more affected by the protonation of ligands than that of AutoDock.
- The AutoDock program gave the most reliable and robust results, both with respect to the accuracy of the docked structures and ranking compounds according to their activity in inhibiting Anthrax-EF.

ACKNOWLEDGMENTS

The authors would like to thank Jennifer Pawlik and Kathryn Bush for their technical assistance with the EF assays, and Dr. Milind Misra for a careful reading of the manuscript.

REFERENCES

1. Morris GM, Goodsell DS, Huey R, Olson AJ. Distributed automated docking of flexible ligands to proteins: parallel applications of AutoDock 2.4. J Comput Aided Mol Des 1996;10:293–304.
2. Morris GM, Goodsell DS, Halliday RS, Huey R, Hart WE, Belew RK, Olson AJ. Automated docking using a Lamarckian genetic algorithm and an empirical binding free energy function. J Comput Chem 1998;19:1639–1662.
3. Venkatachalam CM, Jiang X, Oldfield T, Waldman M. LigandFit: a novel method for the shape-directed rapid docking of ligands to protein active sites. J Mol Graph Model 2003;21:289–307.
4. Bohm HJ. LUDI: rule-based automatic design of new substituents for enzyme inhibitor leads. J Comput Aided Mol Des 1992;6:593–606.
5. Bohm HJ. The development of a simple empirical scoring function to estimate the binding constant for a protein-ligand complex of known three-dimensional structure. J Comput Aided Mol Des 1994;8:243–256.
6. Bohm HJ. Computational tools for structure-based ligand design. Prog Biophys Mol Biol 1996;66:197–210.
7. Bohm HJ. Prediction of binding constants of protein ligands: a fast method for the prioritization of hits obtained from de novo design or 3D database search programs. J Comput Aided Mol Des 1998;12:309–323.
8. Kramer B, Rarey M, Lengauer T. Evaluation of the FLEXX incremental construction algorithm for protein-ligand docking. Proteins 1999;37:228–241.
9. Jones G, Willett P, Glen RC, Leach AR, Taylor R. Development and validation of a genetic algorithm for flexible docking. J Mol Biol 1997;267:727–748.
10. Halgren TA, Murphy RB, Friesner RA, Beard HS, Frye LL, Pollard WT, Banks JL. Glide: a new approach for rapid, accurate docking and scoring, Part 2: Enrichment factors in database screening. J Med Chem 2004;47:1750–1759.
11. Friesner RA, Banks JL, Murphy RB, Halgren TA, Klicic JJ, Mainz DT, Repasky MP, Knoll EH, Shelley M, Perry JK, Shaw DE, Francis P, Shenkin PS. Glide: a new approach for rapid, accurate docking and scoring. I. Method and assessment of docking accuracy. J Med Chem 2004;47:1739–1749.

12. Bissantz C, Folkers G, Rognan D. Protein-based virtual screening of chemical databases. I. Evaluation of different docking/scoring combinations. J Med Chem 2000;43:4759–4767.
13. Ferrara P, Gohlke H, Price DJ, Klebe G, Brooks CLI. Assessing scoring functions for protein-ligand interactions. J Med Chem 2004; 47:3032–3047.
14. Ananthanarayanan VS, Kerman A. Role of metal ions in ligand-receptor interaction: insights from structural studies. Mol Cell Endocrinol 2006;246:53–59.
15. Khandelwal A, Lukacova V, Comez D, Kroll D, Raha S, Balaz S. A combination of docking, QM/MM methods, and MD simulation for binding affinity estimation of metalloprotein ligands. J Med Chem 2005;48:5437–5447.
16. Hu X, Shelver WH. Docking studies of matrix metalloproteinase inhibitors: zinc parameter optimization to improve the binding free energy prediction. J Mol Graph Model 2003;22:115–126.
17. Hu X, Balaz S, Shelver WH. A practical approach to docking of zinc metalloproteinase inhibitors. J Mol Graph Model 2004;22: 293–307.
18. Irwin JJ, Raushel FM, Shoichet BK. Virtual screening against metalloenzymes for inhibitors and substrates. Biochemistry 2005; 44:12316–12328.
19. Liu J, Dai J, Lu M. Zinc-mediated helix capping in a triple-helical protein. Biochemistry 2003;42:5657–5664.
20. Olsen L, Pettersson I, Hemmingsen L, Adolph HW, Jorgensen FS. Docking and scoring of metallo-β-lactamases inhibitors. J Comput Aided Mol Des 2004;18:287–302.
21. Kirton SB, Murray CW, Verdonk ML, Taylor RD. Prediction of binding modes for ligands in the cytochromes P450 and other heme-containing proteins. Proteins 2005;58:836–844.
22. Kontoyianni M, McClellan LM, Sokol GS. Evaluation of docking performance: comparative data on docking algorithms. J Med Chem 2004;47:558–565.
23. Leppla SH. Anthrax toxin edema factor: a bacterial adenylate cyclase that increases cyclic AMP concentrations of eukaryotic cells. Proc Natl Acad Sci USA 1982;79:3162–3166.
24. de Rooij J, Zwartkruis FJ, Verheijen MH, Cool RH, Nijman SM, Wittinghofer A, Bos JL. Epac is a Rap1 guanine-nucleotide-exchange factor directly activated by cyclic AMP. Nature 1998; 396:474–477.
25. Lacy DB, Collier RJ. Structure and function of anthrax toxin. Curr Top Microbiol Immunol 2002;271:61–85.
26. Lacy DB, Mourez M, Fouassier A, Collier RJ. Mapping the anthrax protective antigen binding site on the lethal and edema factors. J Biol Chem 2002;277:3006–3010.
27. Drum CL, Yan SZ, Bard J, Shen YQ, Lu D, Soelaiman S, Grabarek Z, Bohm A, Tang WJ. Structural basis for the activation of anthrax adenylyl cyclase exotoxin by calmodulin. Nature 2002;415:396–402.
28. Shen Y, Zhukovskaya NL, Guo Q, Florian J, Tang WJ. Calcium-independent calmodulin binding and two-metal-ion catalytic mechanism of anthrax edema factor. EMBO J 2005;24:929–941.
29. Hewlett EL, Underhill LH, Cook GH, Manclark CR, Wolff J. A protein activator for the adenylate cyclase of Bordetella pertussis. J Biol Chem 1979;254:5602–5605.
30. Munier H, Bouhss A, Krin E, Danchin A, Gilles AM, Glaser P, Barzu O. The role of histidine 63 in the catalytic mechanism of Bordetella pertussis adenylate cyclase. J Biol Chem 1992;267: 9816–9820.
31. Soelaiman S, Wei BQ, Bergson P, Lee YS, Shen Y, Mrksich M, Shoichet BK, Tang WJ. Structure-based inhibitor discovery against adenylyl cyclase toxins from pathogenic bacteria that cause anthrax and whooping cough. J Biol Chem 2003;278:25990–25997.
32. Shen Y, Guo Q, Zhukovskaya NL, Drum CL, Bohm A, Tang WJ. Structure of anthrax edema factor-calmodulin-adenosine 5′-(α,β-methylene)-triphosphate complex reveals an alternative mode of ATP binding to the catalytic site. Biochem Biophys Res Commun 2004;317:309–314.
33. Shen Y, Zhukovskaya NL, Zimmer MI, Soelaiman S, Bergson P, Wang CR, Gibbs CS, Tang WJ. Selective inhibition of anthrax edema factor by adefovir, a drug for chronic hepatitis B virus infection. Proc Natl Acad Sci USA 2004;101:3242–3247.
34. Guo Q, Shen Y, Zhukovskaya NL, Florian J, Tang WJ. Structural and kinetic analyses of the interaction of anthrax adenylyl cyclase toxin with reaction products cAMP and pyrophosphate. J Biol Chem 2004;279:29427–29435.
35. Schein CH, Zhou B, Oezguen N, Mathura VS, Braun W. Molego-based definition of the architecture and specificity of metal-binding sites. Proteins 2005;58:200–210.
36. Glusker J, Katz A, Bock C. Two-metal binding motifs in protein crystal structures. Struct Chem 2001;12:323–341.
37. Tesmer JJ, Sunahara RK, Johnson RA, Gosselin G, Gilman AG, Sprang SR. Two-metal-ion catalysis in adenylyl cyclase. Science 1999;285:756–760.
38. Peterson JW, King D, Ezell EL, Rogers M, Gessell D, Hoffpauer J, Reuss L, Chopra AK, Gorenstein D. Cholera toxin-induced PGE(2) activity is reduced by chemical reaction with L-histidine. Biochim Biophys Acta 2001;1537:27–41.
39. Brooijmans N, Kuntz ID. Molecular recognition and docking algorithms. Annu Rev Biophys Biomol Struct 2003;32:335–373.
40. Rarey M, Wefing S, Lengauer T. Placement of medium-sized molecular fragments into active sites of proteins. J Comput Aided Mol Des 1996;10:41–54.
41. Koradi R, Billeter M, Wüthrich K. MOLMOL: a program for display and analysis of macromolecular structures. J Mol Graph 1996;14:51–55.
42. Tribolet R, Sigel H. Influence of the protonation degree on the self-association properties of adenosine 5′-triphosphate (ATP). Eur J Biochem 1988;170:617–626.
43. Sigel H, Bianchi E, Corfu N, Kinjo Y, Tribolet R, Martin R. Stabilities and isomeric equilibria in solutions of monomeric metal-ion complexes of guanosine 5′-triphosphate (GTP4-) and inosine 5′-triphosphate (ITP4-) in comparison with those of adenosine 5′-triphosphate (ATP4-). Chem Eur J 2001;7:3729–3737.
44. Harding M. The architecture of metal coordination groups in proteins. Acta Crystallogr D Biol Crystallogr 2004;60:849–859.
45. Bock C, Katz A, Markham G, Glusker J. Manganese as a replacement for magnesium and zinc: functional comparison of the divalent ions. J Am Chem Soc 1999;121:7360–7372.
46. Brautigam C, Steitz TA. Structural and functional insights provided by crystal structures of DNA polymerases and their substrate complexes. Curr Opin Struct Biol 1998;8:54–63.
47. Brautigam C, Aschheim K, Steitz T. Structural elucidation of the binding and inhibitory properties of lanthanide (III) ions at the 3"-5" exonucleolytic active site of the Klenow fragment. Chem Biol 1999;6:901–908.
48. Rulisek L, Vondrasek J. Coordination geometries of selected transition metal ions (Co^{2+}, Ni^{2+}, Cu^{2+}, Zn^{2+}, Cd^{2+}, and Hg^{2+}) in metalloproteins. J Inorg Biochem 1998;71:115–127.
49. de Backer MM, McSweeney S, Lindley PF, Hough E. Ligand-binding and metal-exchange crystallographic studies on shrimp alkaline phosphatase. Acta Crystallogr D Biol Crystallogr 2004;60 (Part 9):1555–1561.
50. Stote RH, Karplus M. Zinc binding in proteins and solution: a simple but accurate nonbonded representation. Proteins 1995;23: 12–31.
51. Hoops SC, Anderson KW, Merz KMJ. Force field design for metalloproteins. J Am Chem Soc 1991;113:8262–8270.
52. Raha K, Merz KMJ. A quantum mechanics-based scoring function: study of zinc ion-mediated ligand binding. J Am Chem Soc 2004;126:1020–1021.
53. Kellenberger E, Rodrigo J, Muller P, Rognan D. Comparative evaluation of eight docking tools for docking and virtual screening accuracy. Proteins 2004;57:225–242.